

Article

Muscle Transcriptome Analysis of Mink at Different Growth Stages Using RNA-Seq

Min Rong^{1,2}, Xiumei Xing^{1,3} and Ranran Zhang^{1,3,*}

¹ Institute of Special Animal and Plant Sciences, Chinese Academy of Agricultural Sciences, Changchun 130112, China; rongmin12@126.com (M.R.); xingxiumei2004@126.com (X.X.)

² Dezhou Animal Husbandry and Veterinary Development Center, Dezhou 253000, China

³ Key Laboratory of Genetics, Breeding and Reproduction of Special Economic Animals, Ministry of Agriculture and Rural Affairs, Changchun 130112, China

* Correspondence: heavenranran@163.com

Simple Summary: The mink is a small and valuable fur animal resource. RNA-seq was utilized to identify key genes associated with the growth and development of mink. Consequently, genes related to embryonic development (*PEG10*, *IGF2*, *NRK*), cell cycle regulation (*CDK6*, *CDC6*, *CDC27*, *CCNA2*), and the FGF family (*FGF2*, *FGF6*, *FGFR2*) exhibited upregulation at 45 days of age in mink. This suggests their potential involvement in early growth and developmental processes. Conversely, genes associated with skeletal muscle development (*PRVA*, *TNNI1*, *TNNI2*, *MYL3*, *MUSTN1*), a negative regulator of the cell cycle gene (*CDKN2C*), and *IGFBP6* were found to be upregulated at 90 days of age in mink, indicating their potential involvement in rapid growth. In summary, our experimental data establish a foundation for the individual selection of larger-sized mink and elucidate the regulatory mechanisms underlying their growth and development.

Abstract: Mink is a kind of small and precious fur animal resource. In this study, we employed transcriptomics technology to analyze the gene expression profile of mink pectoral muscle tissue, thereby elucidating the regulatory mechanisms underlying mink growth and development. Consequently, a total of 25,954 gene expression profiles were acquired throughout the growth and development stages of mink at 45, 90, and 120 days. Among these profiles, 2607 genes exhibited significant differential expression ($|\log_2(\text{fold change})| \geq 2$ and $p_{\text{adj}} < 0.05$). GO and KEGG enrichment analyses revealed that the differentially expressed genes were primarily associated with the mitotic cell cycle process, response to growth factors, muscle organ development, and insulin resistance. Furthermore, GSEA enrichment analysis demonstrated a significant enrichment of differentially expressed genes in the p53 signaling pathway at 45 days of age. Subsequent analysis revealed that genes associated with embryonic development (e.g., *PEG10*, *IGF2*, *NRK*), cell cycle regulation (e.g., *CDK6*, *CDC6*, *CDC27*, *CCNA2*), and the FGF family (e.g., *FGF2*, *FGF6*, *FGFR2*) were all found to be upregulated at 45 days of age in mink, which suggested a potential role for these genes in governing early growth and developmental processes. Conversely, genes associated with skeletal muscle development (*PRVA*, *TNNI1*, *TNNI2*, *MYL3*, *MUSTN1*), a negative regulator of the cell cycle gene (*CDKN2C*), and *IGFBP6* were found to be up-regulated at 90 days of age, suggesting their potential involvement in the rapid growth of mink. In summary, our experimental data provide robust support for elucidating the regulatory mechanisms underlying the growth and development of mink.



Citation: Rong, M.; Xing, X.; Zhang, R. Muscle Transcriptome Analysis of Mink at Different Growth Stages Using RNA-Seq. *Biology* **2024**, *13*, 283. <https://doi.org/10.3390/biology13050283>

Academic Editor: Nina Smolinska

Received: 15 March 2024

Revised: 19 April 2024

Accepted: 19 April 2024

Published: 23 April 2024



Copyright: © 2024 by the authors. Licensee MDPI, Basel, Switzerland. This article is an open access article distributed under the terms and conditions of the Creative Commons Attribution (CC BY) license (<https://creativecommons.org/licenses/by/4.0/>).

Keywords: mink; transcriptomics; muscle development

1. Introduction

The mink (*Neovison vison*) is a small fur-bearing animal renowned as the “King of Fur” due to its high-quality fur, exquisite coloration, and soft yet durable skin. After the introduction of mink in 1956, China has emerged as a leading country for mink breeding,

achieving a fur harvest of 5.79 million pieces in 2022. However, in the absence of a comprehensive genetic breeding program, the responsibility of selection has been entrusted to experienced breeders. The main economic value of mink is their fur, and size is an important indicator of the grade of the fur. Under the same conditions as other indicators, the larger the fur, the higher the price, which directly affects the efficiency of the breeding farm. Furthermore, mink skin size had a strong positive genetic correlation with body length and body weight [1,2], suggesting that body weight and length measured on live animals were reliable indicators of dried fur size. Thus, studying the genetic regulatory mechanisms of mink growth is crucial for the mink breeding industry. In recent years, with the rapid development of sequencing technology, genomics has been widely used in the study of molecular regulation mechanisms of animal growth and development, promoting the process of animal genome selection breeding [3–7]. However, the relevant research on mink is still lagging behind. It was not until 2017 that the first draft of genome assembly for American mink was published, with a size of 2.4 GB [8]. The breeding of mink genomes becomes possible with this advancement. However, due to the lack of chromosome information, the amount of gene annotation, and other shortcomings, the study of the genome level of mink is limited. With the deepening of research and the development of technology, a chromosome-level genome of mink was assembled in 2022, with a size of 2.68 GB [9], which provides a high-quality reference genome for the study of mink growth and development mechanisms and will greatly promote the pace of mink genome selection breeding research.

Transcriptomics plays a pivotal role in functional genomics, facilitating a comprehensive understanding of gene regulation at the transcriptional level, and serving as an efficacious approach to investigate intricate biological phenomena. Currently, numerous scholars have employed transcriptome technology to investigate the growth performance of animals. Shang performed a comparative transcriptome analysis on pigs exhibiting different phenotypes and discovered that 20 genes involved in myoblast differentiation and muscle fiber formation potentially contribute to the postnatal growth rate and body weight of pigs [10]. Wang identified seven growth-related genes through the comparative transcriptome analysis of Muscovy duck ileum tissue, providing a theoretical foundation for investigating the impact of the ileum on duck growth and metabolism [11]. Tang identified 290 and 87 differentially expressed genes associated with growth traits in the comparative transcriptome analysis of pituitary and muscle tissues from large and small geese, respectively [12,13]. Wen performed a comparative transcriptome analysis on muscle tissue from Tibetan sheep at four different growth stages, revealing that the *LIPE*, *LEP*, *ADIPOQ*, *SCD*, and *FASN* genes may modulate muscle fiber type transformation through the AMPK signaling pathway, consequently impacting meat quality [14]. Identifying these key genes related to economic traits will help uncover the molecular mechanisms governing growth and development, facilitating genome-based selective breeding strategies for animals.

In the preliminary study, we generated growth curves for mink, encompassing weight and body length as phenotypic traits. The results showed that the growth rates of weight and body length were relatively fast during the period from 45 to 120 days of age, especially from 45 to 90 days of age [15]. Therefore, in this study, the muscle tissues of silver-blue mink at three different growth stages (45 days, 90 days, and 120 days of age) were used as samples. Transcriptome sequencing technology was employed to identify key genes and signaling pathways related to muscle growth and development in mink, aiming to establish a foundation for the individual selection of larger-sized mink and to elucidate the regulatory mechanisms underlying their growth and development.

2. Materials and Methods

2.1. Samples Selection and Preparation

The silver-blue mink utilized in this study were all provided by Dalian Mingwei Marten Industry Co., Ltd. (Dalian, China). A total of nine male silver-blue mink in three litters with good body condition and a consistent feeding environment were selected

as experimental animals. Each mink was individually housed in a spacious, ventilated cage within a semi-open facility, ensuring optimal comfort and minimal stress. At the ages of 45 days, 90 days, and 120 days, respectively, three male silver-blue mink were chosen from each litter. Euthanasia was performed using carbon monoxide gas following approved protocols to ensure swift and humane death. Immediately after euthanasia, breast muscle was taken using sterile scalpels, cut into small pieces, placed into frozen tubes for rapid freezing with liquid nitrogen, and brought back to the laboratory for storage at -80°C . The experiment was conducted in accordance with the ARRIVE guidelines, and all animal experimental protocols were approved and authorized by the Animal Care and Use Committee of the Institute of Special Animal and Plant Sciences, Chinese Academy of Agricultural Sciences (permit no. ISAPSAEC-2023-032).

2.2. RNA Extraction and Quality Control

Total RNA was extracted from the nine samples using the TRIzol reagent (Invitrogen, Carlsbad, CA, USA) according to the manufacturer's instructions. Subsequently, 1% agarose gels were utilized to monitor RNA degradation and contamination levels. The purity, concentration, and integrity of the isolated RNA were assessed using the NanoPhotometer spectrophotometer (IMPLEN, Westlake Village, CA, USA), Qubit 2.0 Fluorimeter (Life Technologies, Carlsbad, CA, USA) and the Bioanalyzer 2100 system (Agilent Technologies, Santa Clara, CA, USA). Only high-quality RNA samples were utilized for transcriptome library construction.

2.3. Transcriptome Library Construction and Sequencing

The RNA libraries of the mink were generated using the NEBNext Ultra RNA Library Prep Kit for Illumina following the manufacturer's recommendations. Briefly, the poly-A mRNA was isolated using magnetic beads with attached Oligo (dT). First strand cDNA was synthesized using a random hexamer primer and M-MuLV Reverse Transcriptase (RNase H-). Subsequently, second strand cDNA synthesis was performed using DNA Polymerase I and RNase H. To select cDNA fragments of 370~420 bp in length, the library fragments were purified with the AMPure XP system. The index-coded samples were clustered on a cBot Cluster Generation System using TruSeq PE Cluster Kit v3-cBot-HS (Illumina) according to the manufacturer's instructions. The sequencing of the libraries was performed using an Illumina HiSeq platform (Illumina, San Diego, CA, USA), and 150 bp paired-end reads were generated.

2.4. Reads Mapping to the Reference Genome

The raw data in fastq format was initially processed using the fastp software v0.23.2, and the clean data were obtained by filtering the reads with adapter, reads containing poly-N, and low-quality reads from raw data. The calculations of Q20, Q30, and GC content were performed simultaneously on the clean data. All subsequent analyses were conducted exclusively using the high-quality clean data. The paired-end clean reads were aligned to the *Neovison vison* reference genome using the HISAT2 software (version: 2.0.5). The mapped reads of each sample were assembled by StringTie in a reference-based approach for the prediction of novel genes.

2.5. Gene Expression Analysis

In addition, the number of reads mapped to each gene was calculated using the HTSeq software v2.0.5, where the fragments per kilo base million (FPKM) of each gene were measured based on the length of the gene and read count that was mapped to the gene. The DESeq software (version: 1.20.0) was used to screen the differentially expressed genes (DEGs) using the read count data. An adjusted p value (q value) was calculated using Benjamini and Hochberg's approach for controlling the false discovery rate, where genes with $|\log_2(\text{fold change})| \geq 2$ and $q < 0.05$ were considered as DEGs. The enrichment analysis of GO and KEGG pathways was performed with the clusterProfiler package

(version: 3.8.1) in the R software. The local version of the Gene Set Enrichment Analysis (GSEA) analysis tool (version: 3.0) was used to perform GSEA analysis on the GO and KEGG datasets, respectively.

2.6. Quantitative RT-PCR Analysis

The SYBR[®] Premix Ex Taq[™] kit (TaKaRa, Osaka, Japan) was utilized for the performance of a Quantitative RT-PCR (qRT-PCR) assay on a Roche LightCycler480 instrument. The GAPDH gene served as an internal control. Primer sequences used in the experiment are provided in Table 1. The relative mRNA expression level was determined using the $2^{-\Delta\Delta CT}$ method, and the figure was generated using OriginPro 2018.

Table 1. Primers for quantitative real-time PCR.

| Gene | Gene Description | Primers Sequence (from 5' to 3') |
|---------------|---------------------------------|--|
| <i>CDC27</i> | Cell division cycle 27 | F: TCTCCACAATCACACCTCAGATCC R: TTCACGAAGAAGGCTCATCAAACC |
| <i>IGF2</i> | Insulin like growth factor 2 | F: GCCCTTCTGGAGACCTACTGTG R: AGGTGTCGTATTGGAAGAACTTGC |
| <i>MEGF10</i> | Multiple EGF like domains 10 | F: TTCCGAGGCACCACTTGTGTCAG R: CCAGGCAGGCAGTCACAGAG |
| <i>MUSTN1</i> | Musculoskeletal | F: GCCAAGAACCAGGAGATCAAGTC R: TCGGCTGCCACTGAACACC |
| <i>PEG10</i> | Paternally expressed 10 | F: GATGGACATGGACGATCACTCTATG R: TGCGGCGGGCGGATACTG |
| <i>TNNI1</i> | Troponin I1, slow skeletal type | F: GTGGAGGTGGTGGATGAGGAG R: CCCGACGCAGTGGTGGAC |
| <i>MYH3</i> | Myosin heavy chain 3 | F: CGTCCTGGATGATCTACACCTACTC R: TTCTTGCCTCGGTAGCCTTCC |

3. Results

3.1. Overview of the Mink Transcriptome

To systematically identify the expressed mRNA and their spatiotemporal expression profiles during muscle growth and development in mink, cDNA libraries were constructed from breast muscle samples of nine silver-blue mink (Y45_1, Y45_2, Y45_3, Y90_1, Y90_2, Y90_3, Y120_1, Y120_2, Y120_3). A total of 447,484,956 raw reads were generated from nine cDNA libraries. After filtering, approximately 65.66 Gb of high-quality clean bases were obtained (Table 2). Of these, 88.81% of the clean reads were mapped to the *Neovison vison* reference genome, with 85.76% that were uniquely mapped. Ultimately, a total of 25,954 genes were identified, including 1404 novel genes.

Table 2. Summary of the sequencing data of the nine silver-blue mink.

| Samples | Raw Reads | Clean Reads | Clean Bases (Gb) | Total Mapped | Uniquely Mapped |
|---------|------------|-------------|------------------|--------------|-----------------|
| Y45_1 | 46,417,512 | 45,271,560 | 6.79 | 87.79% | 84.94% |
| Y45_2 | 55,331,762 | 54,289,360 | 8.14 | 90.09% | 87.11% |
| Y45_3 | 50,207,396 | 49,355,610 | 7.4 | 89.09% | 86.20% |
| Y90_1 | 50,046,636 | 49,083,374 | 7.36 | 88.26% | 84.96% |
| Y90_2 | 48,711,358 | 47,736,736 | 7.16 | 88.75% | 85.48% |
| Y90_3 | 50,268,714 | 48,472,740 | 7.27 | 87.95% | 85.02% |
| Y120_1 | 48,166,278 | 47,430,618 | 7.11 | 90.19% | 87.36% |
| Y120_2 | 48,847,066 | 47,665,894 | 7.15 | 87.26% | 83.75% |
| Y120_3 | 49,488,234 | 48,537,954 | 7.28 | 89.67% | 86.8% |

The PCA analysis revealed a clear separation among the nine samples, indicating well-defined clusters corresponding to three different time periods (Figure 1A). The squares

of Pearson’s correlation coefficient (R^2) were all greater than 0.92, implying that the samples had a good biological repetition (Figure 1B).

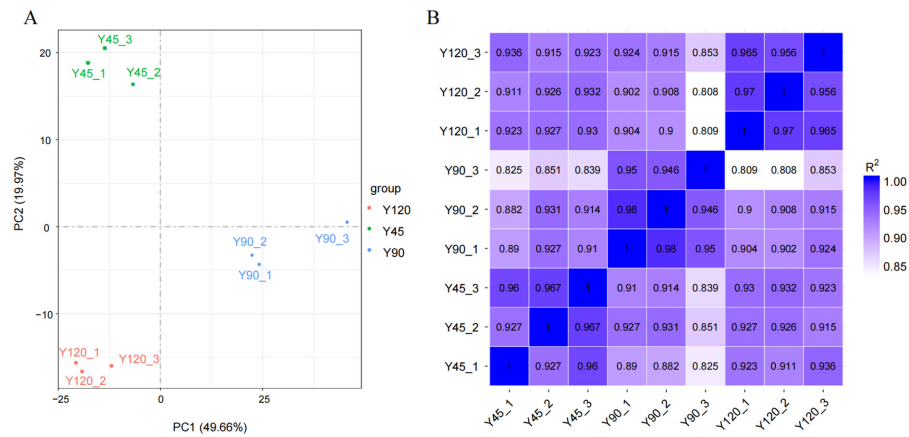


Figure 1. The principal component analysis (A) and correlation analysis (B) for mink muscle.

3.2. Gene Functional Annotation

The gene functional annotation was performed on 25,954 genes, of which 19,992 were successfully annotated into the Gene Ontology (GO) database (Figure 2A). The GO terms primarily encompassed biological processes, such as metabolic processes, biological regulation, and response to stimulus; cellular components, including cell, organelle, organelle part, and macromolecular complex; and molecular functions, such as binding, catalytic activity, and molecular transducer activity.

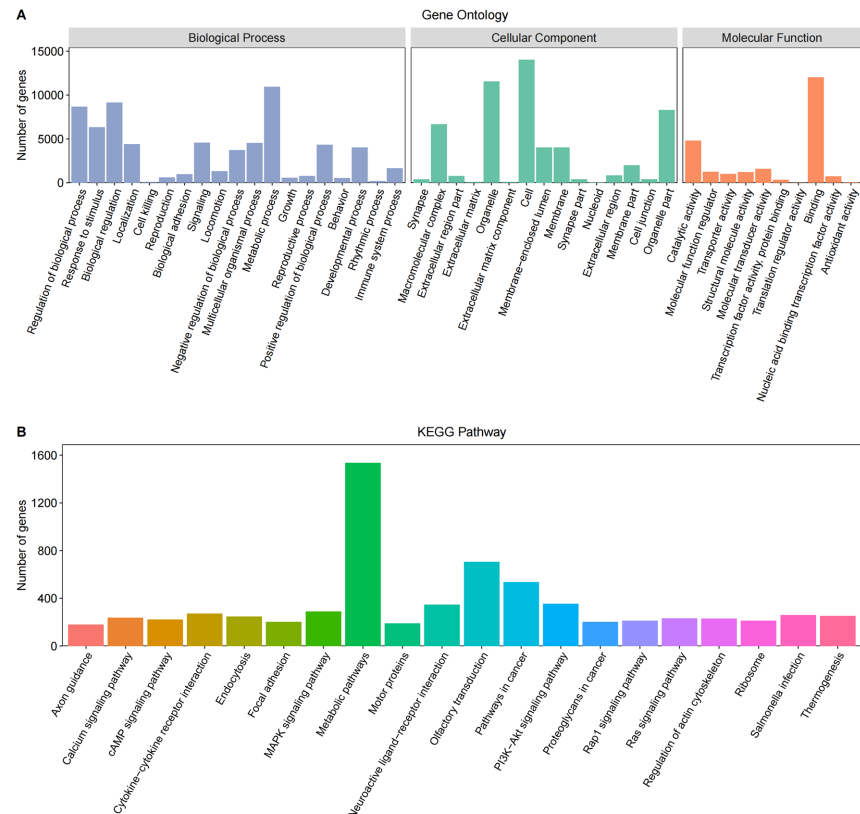


Figure 2. Gene functional annotation based on the Gene Ontology (GO) (A) and Kyoto Encyclopedia of Genes and Genomes (KEGG) (B) pathway databases.

Among the identified genes, 8120 were successfully annotated into the KEGG Pathway database (Figure 2B), mainly including metabolic pathways, olfactory transmission, pathways in cancer, PI3K-Akt signaling pathway, neuroactive ligand-receptor interaction, MAPK signaling pathway, and Cytokine-cytokine receptor interaction.

3.3. Identifying the Differentially Expressed Genes

Through pairwise comparisons of muscle samples from three developmental stages, a total of 2607 genes were identified in terms of $|\log_2(\text{fold change})| \geq 2$ and $p_{\text{adj}} < 0.05$. Specifically, there were 1570 DEGs between Y90 and Y45, 483 DEGs between Y120 and Y45, and 1821 DEGs between Y120 and Y90 (Figure 3A–C, Table S1). The volcano plot revealed a significant up-regulation of *PEG10*, *ARHGAP36*, *IGF2*, *NRK*, and *MYH3* with higher fold changes observed at 45 days of age, whereas *PRVA*, *RIT2*, and *SLC29A2* exhibited decreased expression levels at the same time point. The expression level of *NFAT5* at 90 days of age was observed to be lower compared to that at 45 and 120 days of age, indicating a significant temporal variation in its expression; in contrast, *MUSTN1*, a regulator of bone growth and development, showed the inverse pattern. Subsequently, a Venn diagram analysis was conducted on the DEGs. The intersection of DEGs yielded 14 key genes, including *DLK1*, *FBN2*, *MUSTN1*, *NRK*, *PEG10*, *SLC29A2*, *TFRC*, *TAL7*, *ENSNVIG00000007639*, *ENSNVIG00000009406*, *ENSNVIG00000009488*, *ENSNVIG00000009493*, *ENSNVIG00000020113*, *novel.942* (Figure 3D).

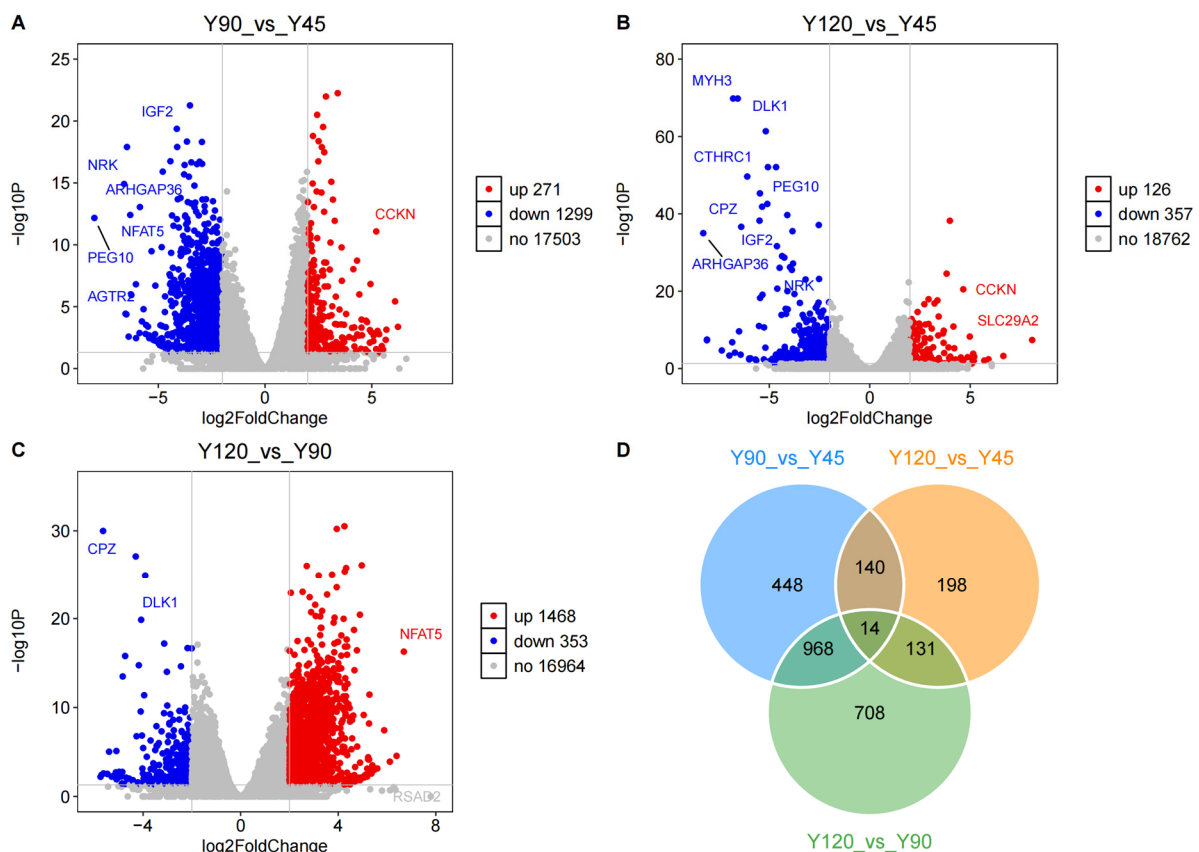


Figure 3. The differential expression genes analysis. (A–C) Gene expression volcano plots for Y90_vs_Y45, Y120_vs_Y45, and Y120_vs_Y90, respectively; (D) The Venn plot of DEGs.

3.4. Functional Analysis of the Differentially Expressed Genes

The function of DEGs was explored using GO enrichment analysis (Table S2, Figure 4A). For the BP category, the top significance terms were mitotic cell cycle process ($p_{\text{adj}} = 4.53 \times 10^{-07}$), response to growth factor ($p_{\text{adj}} = 4.53 \times 10^{-07}$), muscle organ development ($p_{\text{adj}} = 0.00087$). In

the case of the CC category, the most abundant GO terms were cell junction ($p_{\text{adj}} = 6.97 \times 10^{-05}$), mitotic spindle ($p_{\text{adj}} = 6.97 \times 10^{-05}$), transporter complex ($p_{\text{adj}} = 0.0012$); in the MF category, the DEGs mainly involved protein serine/threonine kinase activity ($p_{\text{adj}} = 2.63 \times 10^{-09}$), tubulin binding ($p_{\text{adj}} = 9.26 \times 10^{-06}$), motor activity ($p_{\text{adj}} = 0.00013$), and growth factor binding ($p_{\text{adj}} = 0.00095$).

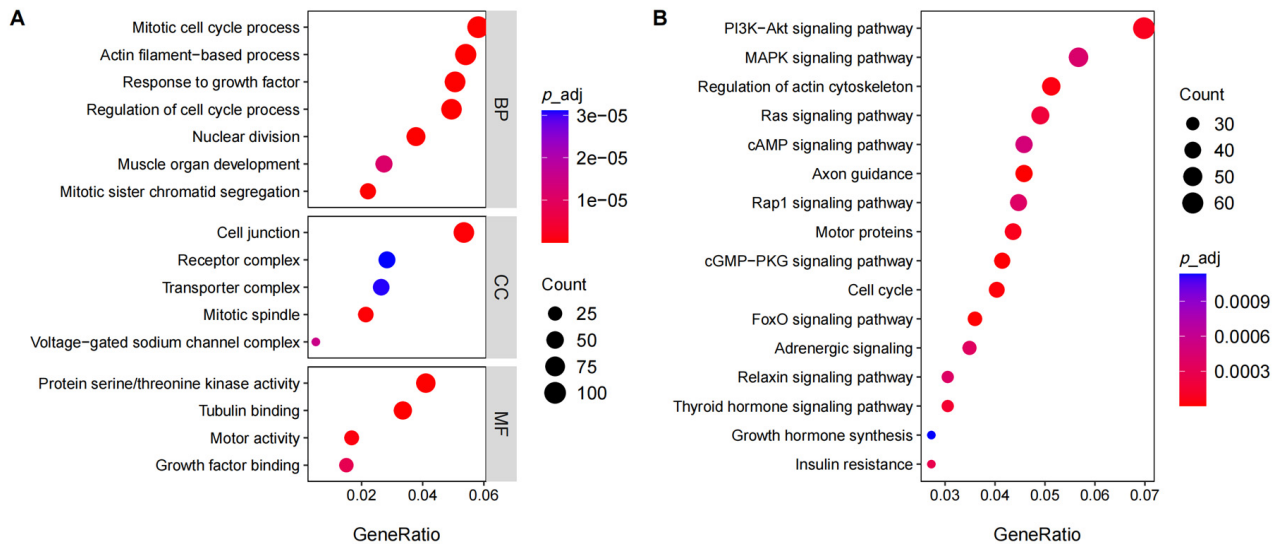


Figure 4. Functional analysis of DEGs. (A): the enrichment GO terms in the three categories (Biological Process, Molecular Function, Cellular Component); (B): The KEGG pathways with significant enrichment.

The KEGG pathways with significant enrichment are presented in Figure 4B, including axon guidance ($p_{\text{adj}} = 3.21 \times 10^{-06}$), FoxO signaling pathway ($p_{\text{adj}} = 8.12 \times 10^{-06}$), cGMP-PKG signaling pathway ($p_{\text{adj}} = 1.13 \times 10^{-05}$), Cell cycle ($p_{\text{adj}} = 2.40 \times 10^{-05}$), regulation of actin cytoskeleton ($p_{\text{adj}} = 3.59 \times 10^{-05}$), motor proteins ($p_{\text{adj}} = 6.95 \times 10^{-05}$), PI3K-Akt signaling pathway ($p_{\text{adj}} = 7.36 \times 10^{-05}$), and insulin resistance ($p_{\text{adj}} = 0.00028$) (Table S3).

In addition to the GO and KEGG enrichment analysis of DEGs, we also performed GSEA-GO and GSEA-KEGG enrichment analysis on all quantitative genes. This comprehensive analysis enabled us to identify the most significantly enriched gene sets in the dataset, providing valuable insights into the cellular processes and pathways most actively involved in the observed cellular functions. The results revealed that the mitotic cell cycle and p53 signaling pathway exhibited enrichment at 45 days of age, while musculoskeletal movement and the ATP metabolic process showed enrichment at 90 days of age. Additionally, the glucagon signaling pathway and autophagy were found to be enriched at 120 days of age (Figure 5, Tables S4 and S5).

3.5. qRT-PCR Validation of DEGs

To further validate the results of RNA-seq, seven DEGs, including cell division cycle 27 (CDC27), insulin like growth factor 2 (IGF2), multiple EGF like domains 10 (MEGF10), musculoskeletal (MUSTN1), paternally expressed 10 (PEG10), troponin I1, slow skeletal type (TNNI1), and myosin heavy chain 3 (MYH3) were selected to perform qRT-PCR. *MUSTN1* and *TNNI1* had higher FPKM in Y90, while *IGF2*, *MEGF10*, *PEG10*, and *MYH3* had higher FPKM in Y45. The relative expression levels of the genes obtained by qRT-PCR, as depicted in Figure 6, exhibited a high degree of concordance with the FPKM values derived from Illumina RNA-seq analysis, thereby confirming the robustness and reliability of the sequencing data.

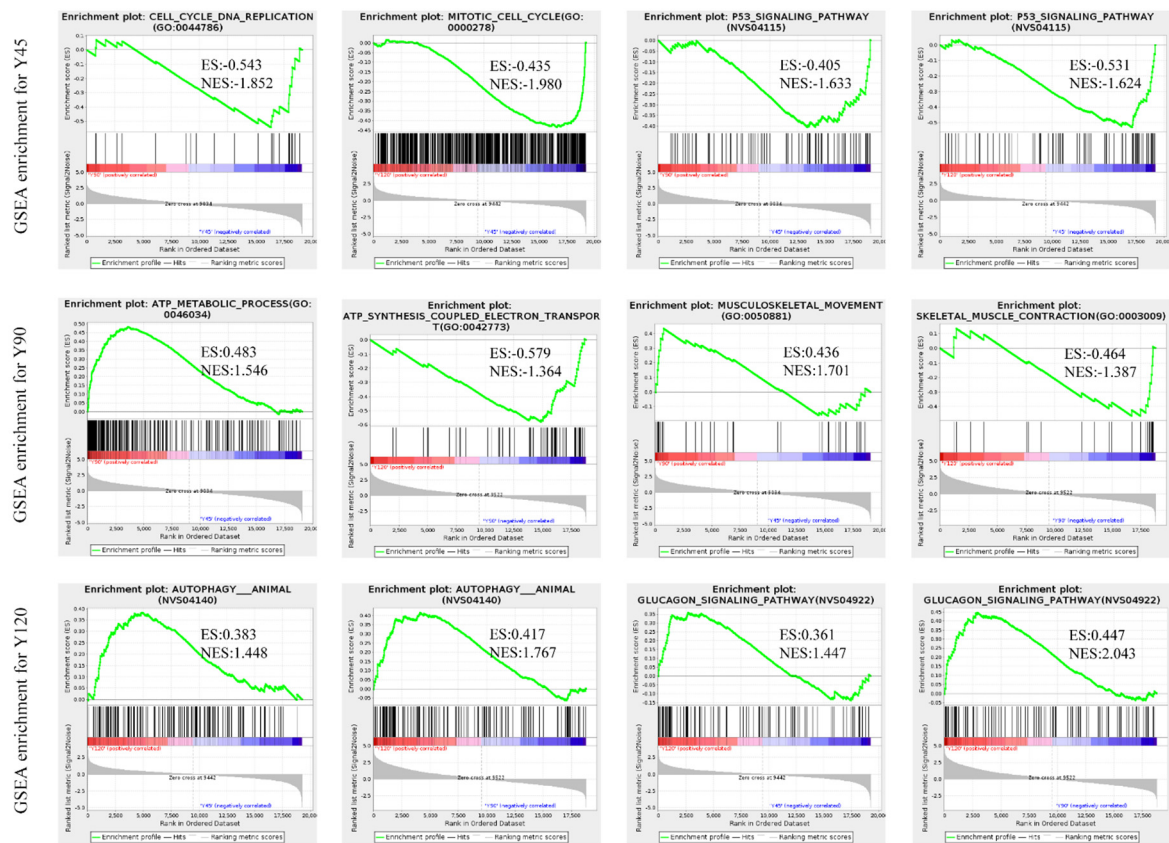


Figure 5. The GSEA analysis result.

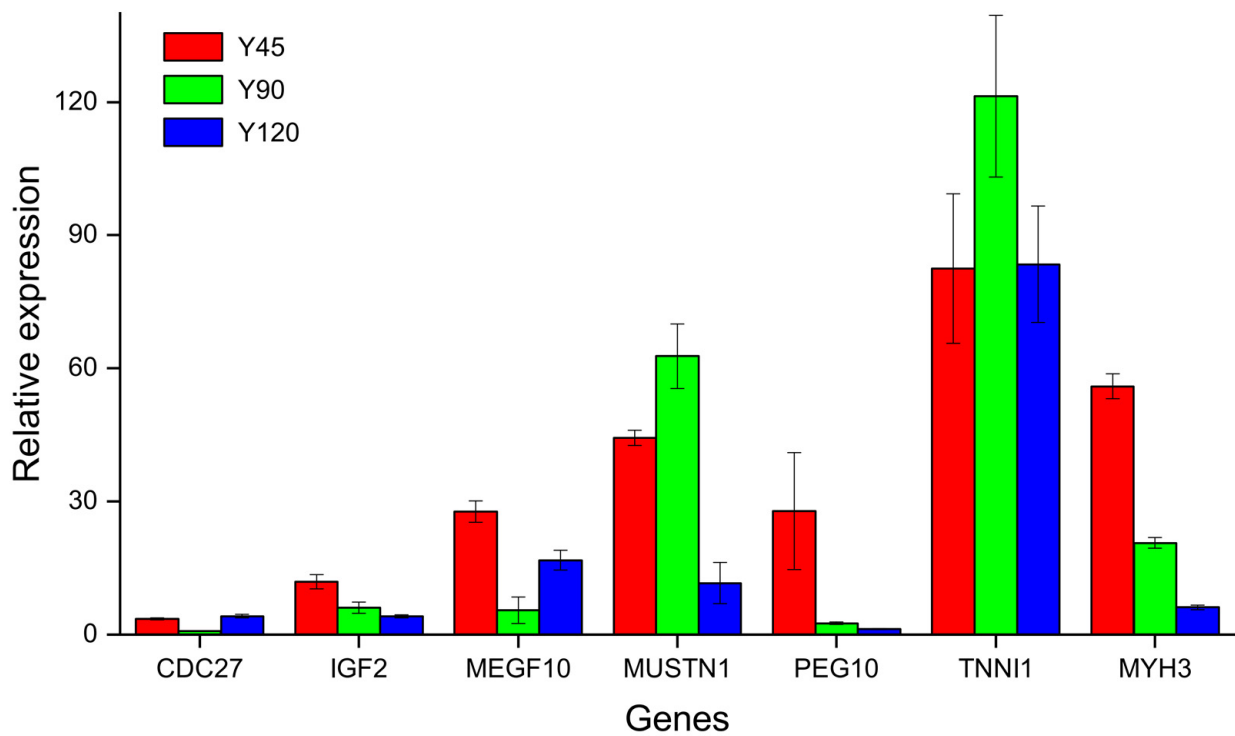


Figure 6. The relative expression levels of seven genes by qRT-PCR.

4. Discussion

This study conducted RNA extraction from breast muscle samples collected from silver-blue mink at 45, 90, and 120 days of age during their rapid growth phase. Subsequently, a comprehensive transcriptome database was established to elucidate the genetic regulation of mink's growth and development.

The expression of 2607 genes showed significant differential regulation, with *PEG10*, *ARHGAP36*, *IGF2*, *NRK*, and *MYH3* exhibiting high foldchange and up-regulation at 45 days of age. Previous studies have demonstrated the crucial roles of *PEG10*, *IGF2*, and *NRK* in embryonic development regulation, characterized by elevated expression levels during the embryonic stage compared to adult individuals [16–20]. This finding enhances our understanding of the up-regulation mechanism of these genes during early mink development. The pivotal role of *IGF2* as a regulator of myogenesis has been widely acknowledged, with its depletion impeding this process [21]. Furthermore, in vitro experiments have demonstrated that a deficiency of *IGF2* within primary skeletal muscle cell-derived myotubes leads to impaired mitochondrial function. However, at 90 days of age, there was a significant increase in the expression levels of *MUSTN1* and *PRVA*, which are crucial genes involved in bone growth and development [22,23]. Therefore, *PEG10*, *IGF2*, and *NRK* are more likely to exert regulatory control over myogenesis during the early postnatal period of mink, while *MUSTN1* is responsible for regulating the proliferation and differentiation of skeletal muscle satellite cells (SMSCs), thereby facilitating skeletal muscle growth. In addition, *DLK1* and *FBN2* were included in a list of 14 shared differentially expressed genes. Furthermore, *DLK1* is an imprinted paternal gene involved in regulating cell growth through encoding a transmembrane protein with multiple epidermal growth factor repeats [24]. It plays a crucial role as a key regulator of mammalian growth and development. Fibrillin-2 (*FBN2*) is a component of connective tissue microfibrils and may be involved in elastic fiber assembly. Its mutations can lead to genetic diseases such as myopathy [25]. The *FBN2* gene has been reported to be associated with height percentile in children and is also a key determinant for skeletal muscle development in Kazakh sheep.

The determination of skeletal muscle fiber numbers primarily occurs during embryonic development, while postnatal changes mainly result from the fusion of muscle satellite cells with fibers, leading to hypertrophy [26]. In the study, 51 DEGs associated with muscle development were identified during the growth and development stages of mink. Notably, *IGF2*, *MYOG*, *MEGF10*, *MYMX*, *MYMK*, *SOX8*, and *PITX1* exhibited upregulated expression at 45 days, with stronger expression in skeletal muscle satellite cells where they play crucial roles in muscle regeneration [7,27,28]. Furthermore, it has been observed that certain genes exhibit a requirement for cooperative interactions in order to ensure their proper functionality. *MYOG* exhibits a similar expression pattern with *MEGF10* and positively regulates *MEGF10* transcription during muscle regeneration; Knockout experiments underscored the indispensable collaboration between *MYMX* and *MYMK* in muscle fiber formation during both embryonic development and adulthood [29,30]. Conversely, *TNNI1*, *TNNI2*, *MYL3*, and *MUSTN1* were up-regulated at day 90, a stage characterized by higher growth rates. It has been demonstrated that *MUSTN1* exhibits the highest expression level during the phase of duck muscle development associated with the maximum relative growth rate [31]. *MYL3*, *TNNI1*, and *TNNI2* have been identified as key regulators of muscle contraction [32,33]. Consequently, these genes are expected to exhibit a positive correlation with the development of breast muscle in mink.

In muscle growth and development, the body precisely regulates the number of cells by regulating key processes such as cell cycle and apoptosis [26]. Cell cycle progression is driven by the dimeric complexes of Cyclin and Cyclin-dependent kinases (CDKs). It is found that at 90 days of age, the genes *ATRX*, *BUB1*, *BUB1B*, *CDK6*, *CDC6*, *CDC27*, *CCNA2*, *E2F2*, *MCM4*, *KNL1*, *RAD21*, and *PPP2R5E* that positively regulate the cell cycle were significantly down-regulated, while *CDKN2C* was up-regulated at this age [34]. It is known that *CDKN2C* is involved in the inhibition of the cell cycle during cell proliferation. Furthermore, we conducted GSEA analysis [35], which primarily focuses on the overall

expression pattern of gene sets rather than being limited to DEGs. It theoretically facilitates the identification of genes that may not exhibit significant differential expression but possess crucial biological significance. The results showed that the p53 signaling pathway was significantly enriched in the tissues of 45-day-old minks. In addition to genes involved in cell cycle regulation, genes involved in apoptosis (*BCL2*, *TP53*, *TP73*, *CDKN1A*, *PERP*, *STEAP3*, *PTEN*, *ZMAT3*, and *MDM2*) were significantly associated with this pathway. Although there was no significant difference in the expression of these genes, they may still play an important role in the development of the pectoral muscle tissues of minks.

Many growth factors and cytokines can affect the proliferation and differentiation of satellite cells. It is widely acknowledged that insulin plays an important role in skeletal muscle growth by regulating muscle hypertrophy, protein accumulation, and cell activity. *INSR* is a tyrosine kinase-like insulin receptor that acts as a molecular switch in insulin signaling [36], and the knockdown of *INSR* induces G1/G0 cell cycle arrest and inhibits cell proliferation [37]. *IGF2*, *IGF2R*, *IGF2BP2*, *IGF2BP3*, and *IGFBP6* have also demonstrated significant influence on animal growth and muscle development [38]. Takashi Saito observed a sharp decline in the expression levels of *IGF1*, *IGF2*, *IGFR1*, *IGFR2*, *IGFBP3*, and *IGFBP5* mRNA in masseter muscle between 14 and 19 days postpartum [39]. A transcriptomic analysis of chicken leg muscle showed that the expression levels of *IGFBP3*, *IGFBP5*, and *IGFBP7* decreased at 16 weeks of age [40]; The aforementioned trend is also evident in the findings of our experiments. *IGFBPs*, a family of six or more related proteins that bind IGF with high affinity, could sequester IGF to decrease protein synthesis and inhibit muscle cell differentiation. The affinity of *IGFBP6* towards *IGF2* surpasses that of other *IGFBPs*, and the expression level of *IGFBP6* mRNA is highest in muscle tissue [41]. Additionally, it could enhance the muscle differentiation process by triggering predominantly the MAPK pathway in the absence of *IGF2* [42]. Therefore, it is speculated that *IGFBP6* regulates the growth of breast muscle independently of *IGF2* during the growth and development of mink. The DEGs also included members of the FGF family, such as *FGF2*, *FGF6*, and *FGFR2*. Notably, *FGF6* is a developmental regulatory gene with highly restricted expression in adulthood that promotes satellite cell proliferation by inducing their entry into the cell cycle [43,44]. The *FGFR2* protein belongs to the fibroblast growth factor receptor family. Its extracellular domain interacts with fibroblast growth factors, initiating a cascade of downstream signals that ultimately regulate mitogenesis and differentiation. Hence, similar to *IGF2*, *FGFs* also tend to play a more important regulatory role in the early growth and development of mink.

5. Conclusions

This study utilized RNA-seq technology and bioinformatics methods to characterize the gene expression profile of silver-blue mink muscle tissue. The results indicate that a total of 25,954 gene expression profiles were obtained during the growth and development stages of mink at 45, 90, and 120 days, with 2607 genes showing significant differential expression. Most differentially expressed genes (DEGs) were associated with the mitotic cell cycle, response to growth factors, muscle organ development, and insulin resistance. Subsequent analysis revealed the upregulation of genes related to embryonic development, cell cycle regulation, and the FGF family at 45 days in mink. Conversely, genes involved in skeletal muscle development and the negative regulation of the cell cycle were found to be upregulated at 90 days. These findings provide valuable insights into the regulatory mechanisms underlying mink growth and development.

Supplementary Materials: The following supporting information can be downloaded at: <https://www.mdpi.com/article/10.3390/biology13050283/s1>, Table S1: List of the identified differentially expressed genes (DEGs); Table S2: GO functional enrichment analysis of differentially expressed genes (DEGs); Table S3: KEGG functional enrichment analysis of differentially expressed genes (DEGs); Table S4: The P53 signaling pathway in Y90_vs_Y45 for GSEA-KEGG analysis; Table S5: The P53 signaling pathway in Y120_vs_Y45 for GSEA-KEGG analysis.

Author Contributions: Methodology, M.R.; software, R.Z.; writing—original draft preparation, R.Z.; writing—review and editing, M.R.; visualization, R.Z.; supervision, X.X.; project administration, X.X.; funding acquisition, M.R. All authors have read and agreed to the published version of the manuscript.

Funding: This research and the APC were funded by Natural Science Foundation of Jilin Province of China, grant number 20210101363JC.

Institutional Review Board Statement: The animal study protocol was approved and authorized by the Animal Care and Use Committee of the Chinese Academy of Agricultural Sciences.

Informed Consent Statement: Not applicable.

Data Availability Statement: Data are contained within the article.

Conflicts of Interest: The authors declare no conflicts of interest.

References

1. Thirstrup, J.P.; Jensen, J.; Lund, M.S. Genetic parameters for fur quality graded on live animals and dried pelts of American mink (*Neovison vison*). *J. Anim. Breed. Genet.* **2017**, *134*, 322–331. [[CrossRef](#)] [[PubMed](#)]
2. Valipour, S.; Karimi, K.; Barrett, D.; Do, D.N.; Hu, G.; Sargolzaei, M.; Wang, Z.; Miar, Y. Genetic and Phenotypic Parameters for Pelt Quality and Body Length and Weight Traits in American Mink. *Animals* **2022**, *12*, 3184. [[CrossRef](#)] [[PubMed](#)]
3. Cendron, F.; Cassandro, M.; Penasa, M. Genome-wide investigation to assess copy number variants in the Italian local chicken population. *J. Anim. Sci. Biotechnol.* **2024**, *15*, 2. [[CrossRef](#)] [[PubMed](#)]
4. Arikawa, L.M.; Mota, L.F.M.; Schmidt, P.I.; Frezarim, G.B.; Fonseca, L.F.S.; Magalhaes, A.F.B.; Silva, D.A.; Carvalheiro, R.; Chardulo, L.A.L.; Albuquerque, L.G. Genome-wide scans identify biological and metabolic pathways regulating carcass and meat quality traits in beef cattle. *Meat Sci.* **2024**, *209*, 109402. [[CrossRef](#)] [[PubMed](#)]
5. Zhao, H.; Sun, G.; Mu, X.; Li, X.; Wang, J.; Zhao, M.; Zhang, G.; Ji, R.; Chen, C.; Gao, G. Genome-wide selective signatures mining the candidate genes for egg laying in goose. *BMC Genom.* **2023**, *24*, 750. [[CrossRef](#)] [[PubMed](#)]
6. Zhang, L.; Zhang, S.; Yuan, M.; Zhan, F.; Song, M.; Shang, P.; Yang, F.; Li, X.; Qiao, R.; Han, X.; et al. Genome-Wide Association Studies and Runs of Homozygosity to Identify Reproduction-Related Genes in Yorkshire Pig Population. *Genes* **2023**, *14*, 2133. [[CrossRef](#)] [[PubMed](#)]
7. Liufu, S.; Lan, Q.; Liu, X.; Chen, B.; Xu, X.; Ai, N.; Li, X.; Yu, Z.; Ma, H. Transcriptome Analysis Reveals the Age-Related Developmental Dynamics Pattern of the Longissimus Dorsi Muscle in Ningxiang Pigs. *Genes* **2023**, *14*, 1050. [[CrossRef](#)] [[PubMed](#)]
8. Cai, Z.; Petersen, B.; Sahana, G.; Madsen, L.B.; Larsen, K.; Thomsen, B.; Bendixen, C.; Lund, M.S.; Guldbrandtsen, B.; Panitz, F. The first draft reference genome of the American mink (*Neovison vison*). *Sci. Rep.* **2017**, *7*, 14564. [[CrossRef](#)] [[PubMed](#)]
9. Karimi, K.; Do, D.N.; Wang, J.; Easley, J.; Borzouie, S.; Sargolzaei, M.; Plastow, G.; Wang, Z.; Miar, Y. A chromosome-level genome assembly reveals genomic characteristics of the American mink (*Neogale vison*). *Commun. Biol.* **2022**, *5*, 1381. [[CrossRef](#)]
10. Shang, P.; Wang, Z.; Chamba, Y.; Zhang, B.; Zhang, H.; Wu, C. A comparison of prenatal muscle transcriptome and proteome profiles between pigs with divergent growth phenotypes. *J. Cell Biochem.* **2019**, *120*, 5277–5286. [[CrossRef](#)]
11. Wang, X.; Xiao, Y.; Yang, H.; Lu, L.; Liu, X.; Lyu, W. Transcriptome Analysis Reveals the Genes Involved in Growth and Metabolism in Muscovy Ducks. *BioMed Res. Int.* **2021**, *2021*, 6648435. [[CrossRef](#)]
12. Tang, J.; Shen, X.; Ouyang, H.; Luo, W.; Huang, Y.; Tian, Y.; Zhang, X. Transcriptome analysis of pituitary gland revealed candidate genes and gene networks regulating the growth and development in goose. *Anim. Biotechnol.* **2022**, *33*, 429–439. [[CrossRef](#)] [[PubMed](#)]
13. Tang, J.; Ouyang, H.; Chen, X.; Jiang, D.; Tian, Y.; Huang, Y.; Shen, X. Comparative Transcriptome Analyses of Leg Muscle during Early Growth between Geese (*Anser cygnoides*) Breeds Differing in Body Size Characteristics. *Genes* **2023**, *14*, 1048. [[CrossRef](#)] [[PubMed](#)]
14. Wen, Y.; Li, S.; Bao, G.; Wang, J.; Liu, X.; Hu, J.; Zhao, F.; Zhao, Z.; Shi, B.; Luo, Y. Comparative Transcriptome Analysis Reveals the Mechanism Associated With Dynamic Changes in Meat Quality of the Longissimus Thoracis Muscle in Tibetan Sheep at Different Growth Stages. *Front. Vet. Sci.* **2022**, *9*, 926725. [[CrossRef](#)] [[PubMed](#)]
15. Rong, M.; Tu, J.; Xu, J. Comparison of growth and development and study on fit-ting of growth curves in different colored minks. *Heilongjiang Anim. Sci. Vet. Med.* **2018**, *9*, 184–186. [[CrossRef](#)]
16. Kawai, Y.; Imada, K.; Akamatsu, S.; Zhang, F.; Seiler, R.; Hayashi, T.; Leong, J.; Beraldi, E.; Saxena, N.; Kretschmer, A.; et al. Paternally Expressed Gene 10 (PEG10) Promotes Growth, Invasion, and Survival of Bladder Cancer. *Mol. Cancer Ther.* **2020**, *19*, 2210–2220. [[CrossRef](#)] [[PubMed](#)]
17. Zhu, Y.; Gui, W.; Tan, B.; Du, Y.; Zhou, J.; Wu, F.; Li, H.; Lin, X. IGF2 deficiency causes mitochondrial defects in skeletal muscle. *Clin. Sci.* **2021**, *135*, 979–990. [[CrossRef](#)] [[PubMed](#)]
18. Denda, K.; Nakao-Wakabayashi, K.; Okamoto, N.; Kitamura, N.; Ryu, J.Y.; Tagawa, Y.I.; Ichisaka, T.; Yamanaka, S.; Komada, M. Nrk, an X-linked protein kinase in the germinal center kinase family, is required for placental development and fetoplacental induction of labor. *J. Biol. Chem.* **2011**, *286*, 28802–28810. [[CrossRef](#)] [[PubMed](#)]

19. Kanai-Azuma, M.; Kanai, Y.; Okamoto, M.; Hayashi, Y.; Yonekawa, H.; Yazaki, K. Nrk: A murine X-linked NIK (Nck-interacting kinase)-related kinase gene expressed in skeletal muscle. *Mech. Dev.* **1999**, *89*, 155–159. [[CrossRef](#)]
20. Monk, D.; Sanches, R.; Arnaud, P.; Apostolidou, S.; Hills, F.A.; Abu-Amero, S.; Murrell, A.; Friess, H.; Reik, W.; Stanier, P.; et al. Imprinting of IGF2 P0 transcript and novel alternatively spliced INS-IGF2 isoforms show differences between mouse and human. *Hum. Mol. Genet.* **2006**, *15*, 1259–1269. [[CrossRef](#)]
21. Zanou, N.; Gailly, P. Skeletal muscle hypertrophy and regeneration: Interplay between the myogenic regulatory factors (MRFs) and insulin-like growth factors (IGFs) pathways. *Cell Mol. Life Sci.* **2013**, *70*, 4117–4130. [[CrossRef](#)] [[PubMed](#)]
22. Hu, Z.; Xu, H.; Lu, Y.; He, Q.; Yan, C.; Zhao, X.; Tian, Y.; Yang, C.; Zhang, Z.; Qiu, M.; et al. MUSTN1 is an indispensable factor in the proliferation, differentiation and apoptosis of skeletal muscle satellite cells in chicken. *Exp. Cell Res.* **2021**, *407*, 112833. [[CrossRef](#)]
23. Ayuso, M.; Fernandez, A.; Nunez, Y.; Benitez, R.; Isabel, B.; Fernandez, A.I.; Rey, A.I.; Gonzalez-Bulnes, A.; Medrano, J.F.; Canovas, A.; et al. Developmental Stage, Muscle and Genetic Type Modify Muscle Transcriptome in Pigs: Effects on Gene Expression and Regulatory Factors Involved in Growth and Metabolism. *PLoS ONE* **2016**, *11*, e0167858. [[CrossRef](#)] [[PubMed](#)]
24. Lucifero, D.; Chaillet, J.; Trasler, J. Potential significance of genomic imprinting defects for reproduction and assisted reproductive technology. *Hum. Reprod. Update* **2004**, *10*, 3–18. [[CrossRef](#)]
25. Xu, F.; Jiang, W.; Zhang, T.; Jiang, Q.; Zhang, R.; Bi, H. Fibrillin-2 gene mutations associated with hereditary connective tissue diseases. *Hereditas* **2019**, *41*, 919–927. [[CrossRef](#)]
26. Li, D.; Pan, Z.; Zhang, K.; Yu, M.; Yu, D.; Lu, Y.; Wang, J.; Zhang, J.; Zhang, K.; Du, W. Identification of the Differentially Expressed Genes of Muscle Growth and Intramuscular Fat Metabolism in the Development Stage of Yellow Broilers. *Genes* **2020**, *11*, 244. [[CrossRef](#)]
27. Ito, N.; Kii, I.; Shimizu, N.; Tanaka, H.; Takeda, S. Direct reprogramming of fibroblasts into skeletal muscle progenitor cells by transcription factors enriched in undifferentiated subpopulation of satellite cells. *Sci. Rep.* **2017**, *7*, 8097. [[CrossRef](#)] [[PubMed](#)]
28. Schmidt, K.; Glaser, G.; Wernig, A.; Wegner, M.; Rosorius, O. Sox8 is a specific marker for muscle satellite cells and inhibits myogenesis. *J. Biol. Chem.* **2003**, *278*, 29769–29775. [[CrossRef](#)] [[PubMed](#)]
29. Park, S.Y.; Yun, Y.; Kim, M.J.; Kim, I.S. Myogenin is a positive regulator of MEGF10 expression in skeletal muscle. *Biochem. Biophys. Res. Commun.* **2014**, *450*, 1631–1637. [[CrossRef](#)]
30. Bi, P.; McAnally, J.R.; Shelton, J.M.; Sanchez-Ortiz, E.; Bassel-Duby, R.; Olson, E.N. Fusogenic micropeptide Myomixer is essential for satellite cell fusion and muscle regeneration. *Proc. Natl. Acad. Sci. USA* **2018**, *115*, 3864–3869. [[CrossRef](#)]
31. Xu, T.S.; Gu, L.H.; Sun, Y.; Zhang, X.H.; Ye, B.G.; Liu, X.L.; Hou, S.S. Characterization of MUSTN1 gene and its relationship with skeletal muscle development at postnatal stages in Pekin ducks. *Genet Mol. Res.* **2015**, *14*, 4448–4460. [[CrossRef](#)]
32. Shi, B.; Shi, X.; Zuo, Z.; Zhao, S.; Zhao, Z.; Wang, J.; Zhou, H.; Luo, Y.; Hu, J.; Hickford, J.G.H. Identification of differentially expressed genes at different post-natal development stages of longissimus dorsi muscle in Tianzhu white yak. *Gene* **2022**, *823*, 146356. [[CrossRef](#)] [[PubMed](#)]
33. Li, Y.; Zhou, T.; Zhuang, J.; Dai, Y.; Zhang, X.; Bai, S.; Zhao, B.; Tang, X.; Wu, X.; Chen, Y. Effects of feeding restriction on skeletal muscle development and functional analysis of TNN1 in New Zealand white rabbits. *Anim. Biotechnol.* **2023**, *34*, 4435–4447. [[CrossRef](#)] [[PubMed](#)]
34. Zhang, J.; Suh, Y.; Choi, Y.M.; Chen, P.R.; Davis, M.E.; Lee, K. Differential Expression of Cell Cycle Regulators During Hyperplastic and Hypertrophic Growth of Broiler Subcutaneous Adipose Tissue. *Lipids* **2015**, *50*, 965–976. [[CrossRef](#)]
35. Subramanian, A.; Tamayo, P.; Mootha, V.K.; Mukherjee, S.; Ebert, B.L.; Gillette, M.A.; Paulovich, A.; Pomeroy, S.L.; Golub, T.R.; Lander, E.S.; et al. Gene set enrichment analysis: A knowledge-based approach for interpreting genome-wide expression profiles. *Proc. Natl. Acad. Sci. USA* **2005**, *102*, 15545–15550. [[CrossRef](#)]
36. Lee, J.; Pilch, P.F. The insulin receptor: Structure, function, and signaling. *Am. J. Physiol.* **1994**, *266*, C319–C334. [[CrossRef](#)] [[PubMed](#)]
37. Wei, W.; Zhang, W.Y.; Bai, J.B.; Zhang, H.X.; Zhao, Y.Y.; Li, X.Y.; Zhao, S.H. The NF-kappaB-modulated microRNAs miR-195 and miR-497 inhibit myoblast proliferation by targeting Igf1r, Insr and cyclin genes. *J. Cell Sci.* **2016**, *129*, 39–50. [[CrossRef](#)] [[PubMed](#)]
38. Florini, J.R.; Ewton, D.Z.; Coolican, S.A. Growth hormone and the insulin-like growth factor system in myogenesis. *Endocr. Rev.* **1996**, *17*, 481–517. [[CrossRef](#)]
39. Saito, T.; Akutsu, S.; Urushiyama, T.; Ishibashi, K.; Nakagawa, Y.; Shuler, C.F.; Yamane, A. Changes in the mRNA expressions of insulin-like growth factors, their receptors, and binding proteins during the postnatal development of rat masseter muscle. *Zool. Sci.* **2003**, *20*, 441–447. [[CrossRef](#)]
40. Xue, Q.; Zhang, G.; Li, T.; Ling, J.; Zhang, X.; Wang, J. Transcriptomic profile of leg muscle during early growth in chicken. *PLoS ONE* **2017**, *12*, e0173824. [[CrossRef](#)]
41. Zhan, S.Y.; Chen, L.; Li, L.; Wang, L.J.; Zhong, T.; Zhang, H.P. Molecular characterization and expression patterns of insulin-like growth factor-binding protein genes in postnatal Nanjiang brown goats. *Genet. Mol. Res.* **2015**, *14*, 12547–12560. [[CrossRef](#)] [[PubMed](#)]
42. Aboalola, D.; Han, V.K.M. Insulin-Like Growth Factor Binding Protein-6 Promotes the Differentiation of Placental Mesenchymal Stem Cells into Skeletal Muscle Independent of Insulin-Like Growth Factor Receptor-1 and Insulin Receptor. *Stem. Cells Int.* **2019**, *2019*, 9245938. [[CrossRef](#)] [[PubMed](#)]

43. deLapeyriere, O.; Ollendorff, V.; Planche, J.; Ott, M.O.; Pizette, S.; Coulier, F.; Birnbaum, D. Expression of the Fgf6 gene is restricted to developing skeletal muscle in the mouse embryo. *Development* **1993**, *118*, 601–611. [[CrossRef](#)] [[PubMed](#)]
44. Kastner, S.; Elias, M.C.; Rivera, A.J.; Yablonka-Reuveni, Z. Gene expression patterns of the fibroblast growth factors and their receptors during myogenesis of rat satellite cells. *J. Histochem. Cytochem.* **2000**, *48*, 1079–1096. [[CrossRef](#)] [[PubMed](#)]

Disclaimer/Publisher’s Note: The statements, opinions and data contained in all publications are solely those of the individual author(s) and contributor(s) and not of MDPI and/or the editor(s). MDPI and/or the editor(s) disclaim responsibility for any injury to people or property resulting from any ideas, methods, instructions or products referred to in the content.